Plasma penetration of the dayside magnetopause

H. Gunell,[1,a)] H. Nilsson,[2] G. Stenberg,[2] M. Hamrin,[3] T. Karlsson,[4] R. Maggiolo,[1] M. André,[5]
R. Lundin,[2] and I. Dandouras[6]

[1]*Belgian Institute for Space Aeronomy, Avenue Circulaire 3, B-1180 Brussels, Belgium*
[2]*Swedish Institute of Space Physics, P.O. Box 812, SE-981 28 Kiruna, Sweden*
[3]*Department of Physics, Umeå University, SE-901 87 Umeå, Sweden*
[4]*Space and Plasma Physics, Royal Institute of Technology (KTH), SE-100 44 Stockholm, Sweden*
[5]*Swedish Institute of Space Physics, Box 537, SE-751 21 Uppsala, Sweden*
[6]*Institut de Recherche en Astrophysique et Planétologie, UPS-CNRS, Toulouse, France*

Data from the Cluster spacecraft during their magnetopause crossing on 25 January 2002 are presented. The magnetopause was in a state of slow non-oscillatory motion during the observational period. Coherent structures of magnetosheath plasma, here typified as plasmoids, were seen on closed magnetic field lines on the inside of the magnetopause. Using simultaneous measurements on two spacecraft, the inward motion of the plasmoids is followed from one spacecraft to the next, and it is found to be in agreement with the measured ion velocity. The plasma characteristics and the direction of motion of the plasmoids show that they have penetrated the magnetopause, and the observations are consistent with the concept of impulsive penetration, as it is known from theory, simulations, and laboratory experiments. The mean flux across the magnetopause observed was 0.2%–0.5% of the solar wind flux at the time, and the peak values of the flux inside the plasmoids reached approximately 20% of the solar wind flux. © *2012 American Institute of Physics.*
[http://dx.doi.org/10.1063/1.4739446]

I. INTRODUCTION

In magnetospheric physics, an important field of study is the interaction between the magnetopause and the solar wind in which the magnetosphere is immersed. Of particular interest is the entry of solar wind plasma into the magnetosphere, because it populates the magnetosphere and participates in the coupling of solar wind energy to the magnetosphere, where the energy, ultimately, drives phenomena like magnetic storms and the aurora.[1]

Observational studies of how solar wind plasma enters the magnetosphere generally involve analysis of data from spacecraft crossing the magnetopause. When data are available only along the trajectory of a single spacecraft, it is impossible to determine whether the magnetopause is oscillating in position or whether it is stationary or in a slow uniform motion. Observed fluctuations can thus be interpreted either as an observational effect, due to magnetopause oscillations, or as a true plasma phenomenon of importance in plasma transport across the magnetopause. With simultaneous measurements by multiple spacecraft, it becomes possible to distinguish between these different cases.

In this paper, we examine data recorded by the Cluster spacecraft on 25 January 2002, as they moved from inside the magnetosphere across the magnetopause and into the magnetosheath. Data from this magnetopause crossing have been analysed before by Fear *et al.*[2] Those authors considered the several spacecraft one by one and came to the conclusion that the spacecraft approached the boundary intermittently due to oscillations in the magnetopause position. By analysing

simultaneous measurements by two of the spacecraft, we come to the opposite conclusion that the magnetopause was moving slowly and monotonously and that the fluctuations that were observed were caused by plasma structures moving, not only in the spacecraft frame of reference but also in the magnetopause frame of reference. This difference in interpretation has consequences for how we interpret the results in terms of magnetosheath plasma entry into the magnetosphere.

Magnetic reconnection is often invoked to explain solar wind plasma entry into the magnetosphere,[3–7] but there are other processes as well. It has been shown that the Kelvin-Helmholtz instability can be responsible for plasma traversing the magnetopause at the terminator and further downstream in the tail,[8] where the Kelvin-Helmholtz instability reaches its non-linear stage and secondary instabilities provide transport of plasma. Another process, called impulsive penetration, was suggested in the 1970s.[9] In impulsive penetration, inhomogeneities (or plasmoids) with higher momentum density than the surrounding plasma can enter the magnetosphere as filaments. The term plasmoid was first used in laboratory plasma physics by Bostick,[10] and we shall use it in the sense "a coherent mass of plasma."[11] As a plasmoid, with velocity $\mathbf{v}$, enters the stronger geomagnetic field $\mathbf{B}$, ions and electrons gyrate in opposite directions, and space charge layers form on the sides of the plasmoid creating an electric field $\mathbf{E} = -\mathbf{v} \times \mathbf{B}$ inside it. This polarization allows the charged particles to continue moving with their original velocity through the means of an $\mathbf{E} \times \mathbf{B}$-drift.[12,13] Plasmoids with high kinetic energy density can penetrate ballistically by expelling the ambient magnetic field from the interior of the plasmoid.[14] This phase is then followed by a magnetic diffusion phase, in which the plasmoid is magnetized by the

ambient field, and finally the plasmoid can $\mathbf{E} \times \mathbf{B}$-drift as described above.

The impulsive penetration mechanism was first studied in the laboratory, before it was suggested that it could be applied to magnetopause physics, and both experiments and theory have contributed to the understanding of this phenomenon. In the 1950s, it was found experimentally that a plasmoid can move across a magnetic field.[10] Theory for penetration via polarization showed that unless the kinetic energy density of the plasma $W_K = \frac{1}{2} n_e m_i v^2$ is much greater than the energy $W_E = \frac{1}{2} \epsilon_0 (vB)^2$ of the polarization field, this field cannot be set up and penetration is prevented.[12] The quotient W_K/W_E is an approximation of the dielectric constant $\epsilon = 1 + W_K/W_E$. A refined requirement, $\epsilon \gtrsim 10\sqrt{m_i/m_e}$, was later found experimentally.[15] Experimental studies showed that plasmoids can penetrate magnetic fields, while the relative change of the magnetic field, caused by the plasmoid, remains small even for large values of the kinetic beta $\beta_k = W_K/(0.5\mu_0 B^2)$.[14] Experiments with laser produced plasmas have shown that wide plasmoids can break up into smaller plasmoids as they move across the field,[16] and this has been attributed to the Rayleigh-Taylor instability.[17] In active space experiments, where ion beams were injected in the ionosphere, both polarization fields and magnetic field-aligned electric fields were observed.[18] Theory with application to the magnetopause was developed further including the effects of magnetic field gradients.[19] More recent work includes kinetic theory[20] of plasmoid propagation in magnetic fields, and also particle-in-cell simulations and laboratory experiments[21–24] on waves in the lower hybrid frequency range in penetrating plasmoids. Such waves have also been observed at the magnetopause.[25]

Previous space observations inside the dayside magnetopause have shown plasma with characteristics of the magnetosheath.[26,27] There have been observations in the magnetosheath of plasma structures that potentially could penetrate the magnetopause. Hubert *et al.*[28] reported small scale structures related to mirror waves in the magnetosheath. High energy density jets that are thought to be accelerated through a Fermi-type mechanism were observed in the magnetosheath by Savin *et al.*[29] Such jets have been shown to be deflected toward the magnetopause, where they may constitute a source of penetrating plasma.[30] Recently, magnetopause deformation by supermagnetosonic plasma streams has been reported.[31] Hietala *et al.*[32] observed several jets in the magnetosheath during a period when the interplanetary magnetic field was directed outward from the sun. These jets had speeds a few times above that of the ambient magnetosheath plasma. Karlsson *et al.*[33] performed an observational study of 56 plasmoids in the magnetosheath each with a maximum density at least 50% above the density of the surrounding plasma. They found plasmoids in a size range between $0.1 R_E$ and $10 R_E$. There were examples both of plasmoids with a higher velocity, in the anti-sunward direction, than the surrounding magnetosheath plasma and of plasmoids moving with the same velocity as that plasma. A related process has been observed on the nightside, where a sub-auroral ion drift channel is formed when the plasma sphere short circuits a plasmoid, which has been injected in connection with a substorm.[34]

In this paper, we show that plasmoids do penetrate the dayside magnetopause. This is done by observing the plasmoids using data from the Cluster spacecraft; tracing their motion deeper into the magnetosphere from one spacecraft to the next; using simultaneous measurements on two spacecraft to show that the plasmoids were detached from the magnetopause; and by computing a net flux of plasma across the magnetopause. In Sec. II, a general description of the data, the solar wind, and magnetopause conditions is given. In Sec. III, we analyse the plasmoid motion using simultaneous measurements on two of the spacecraft. In Sec. IV, the particle flux across the magnetopause is computed. In Sec. V, we consider the possibility of the magnetopause being a rotational discontinuity. In Sec. VI, the plasmoid size is estimated from data and compared to theoretical estimates. In Sec. VII, we discuss the conclusions and interpretations of the measurements.

II. MEASUREMENTS

We present data from the Cluster spacecraft on 25 January 2002 between 10:10 and 11:00 UT. We restrict our analysis to Cluster spacecraft 1, 3, and 4, for which there are CIS (Cluster ion spectrometry) data. The spacecraft were located on the dayside of the earth and moved from inside the magnetosphere, across the magnetopause, into the magnetosheath. The Cluster spacecraft crossed the magnetopause at a position $(x, y, z) \approx (3.4, 6.6, 8.5) R_E$ in geocentric solar ecliptic (GSE) coordinates. The time of crossing was 10:46 for Cluster 1 and 4 and 10:41 for Cluster 3. Fig. 1 shows the orbit of the Cluster spacecraft. The two top panels show the projection of the orbit onto the x–y and x–z planes in GSE coordinates. The bottom panels show the orbit in cylindrical coordinates, the horizontal axis being the GSE x-axis, and the vertical axis showing the distance to the x-axis. The bottom right panel shows a closeup of the spacecraft orbits, with their positions marked at the time Cluster 3 crossed the magnetopause. The magnetopause that is shown in all four panels is a Shue model[35] magnetopause that has been scaled to fit the observed crossing by Cluster 3. The solar wind parameters were measured by the magnetic field investigation (MFI)[36] and the solar wind experiment (SWE)[37] instruments on-board the Wind spacecraft. The solar wind proton density, speed, and magnetic field are shown in Fig. 2. The Wind spacecraft was located at $(x, y, z) \approx (22, -321, 18) R_E$, which means that, at the measured solar wind speed, its location was 7 min upstream. Assuming that the solar wind conditions did not change appreciably over the $321 R_E$ displacement in the negative y-direction it should provide relevant parameters. Mean values obtained between 10:10 and 11:00 are shown in Table I. The density and speed curves were quite uneventful during this period. The magnitude of the magnetic field was also nearly constant, whereas there are some changes in the magnetic field direction. For the period that is under analysis here, that is to say, between 10:10 and 11:00 the interplanetary magnetic field was close
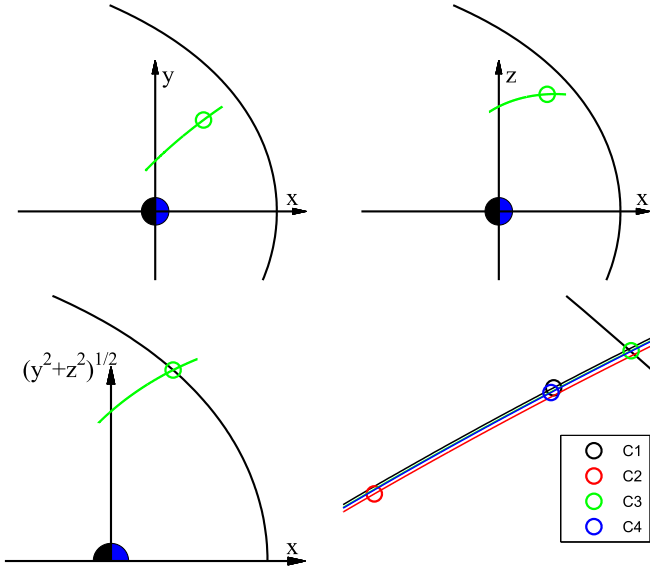
FIG. 1. Orbit of the Cluster spacecraft on 25 January 2002. The top left panel shows the orbit of Cluster 3 in GSE coordinates, projected onto the *x*–*y* plane; the top right shows a projection on the *x*–*z* plane; the bottom left panel shows the Cluster 3 orbit in cylindrical coordinates; and the bottom right panel shows a closeup of the spacecraft orbits near the magnetopause in cylindrical coordinates. The position of the magnetopause crossing of Cluster 3 is marked by green circles in all panels, and the positions of the other spacecraft at that same instant are shown the bottom right panels as black, red, and blue circles for Cluster 1, 2, and 4, respectively. A Shue model magnetopause, which has been scaled to agree with the observed Cluster 3 magnetopause crossing, is shown in black in all panels. Specifically, what is shown in the upper panels is the intersection of the magnetopause with the plane of the figure. That is why the green circle, which shows the projection of the magnetopause crossing onto that plane, does not lie on the curve showing the magnetopause.

to the ecliptic plane and directed toward negative *y*, in GSE coordinates.

Fig. 3 shows the magnetic field observed by the FGM (fluxgate magnetometer)[38] instrument on Cluster 1, 3, and 4 in panels (a), (b), and (c), respectively. Panels (g), (h), and (i) show the ion velocity. At the start of the interval shown,
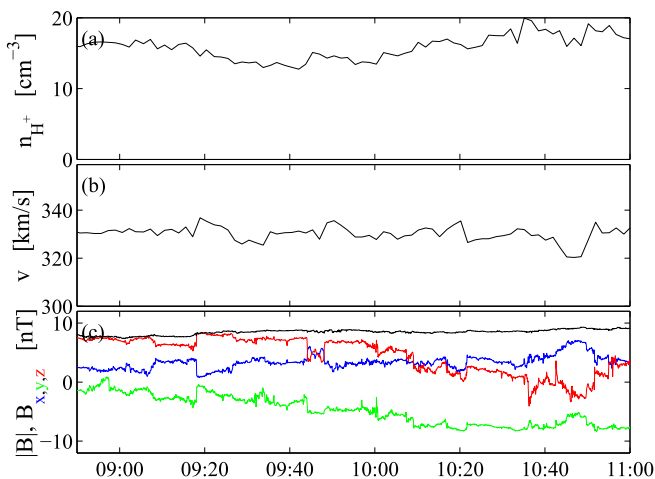

FIG. 2. Solar wind parameters measured by the Wind spacecraft. Panel (a) shows the proton density; (b) the solar wind speed; and (c) the magnetic field magnitude $|\mathbf{B}|$ (black), and the GSE B_x (blue), B_y (green), and B_z (red) components.

TABLE I. Solar wind parameters from the Wind spacecraft.

Magnetic field B	$(4.0, -7.4, 0.98)$ nT
Velocity $\mathbf{v}_{SW}$	$(-325, -50.2, 3.1)$ km/s
Speed v_{SW}	329 km/s
Proton density	1.7×10^7 m^{-3}
Proton flux	5.7×10^{12} m^{-2}s^{-1}

the spacecraft are inside the magnetosphere, moving outward. At the time that has been marked with a vertical dashed line (10:31 for spacecraft 3 and 10:37 for spacecrafts 1 and 4) a transition region is reached, where the plasma velocity starts to change toward magnetosheath values. The magnetic field direction remains more or less unchanged until the time marked by the solid vertical line (10:41 for Cluster 3 and 10:46 for Cluster 1 and 4), where $\mathbf{B}_x$ changes sign from negative to positive, and the spacecraft enter the magnetosheath.

Fig. 4 shows the electron and proton energy spectra for Cluster 1, 3, and 4. The ion spectra are summed over all pitch angles, whereas the electron spectra are the sum of the first and last pitch angle bins only, that is to say, pitch angles in the ranges [0°, 15°] and [165°, 180°] are included. We chose to show the electrons in this way because the presence of a hot field-aligned electron population can be used to diagnose the magnetic field configuration.[39] The dashed and solid vertical lines mark the inner and outer boundaries of the transition region, respectively, as in Fig. 3. The ion spectra were measured by the CIS instruments[40] and the electron spectra by the PEACE (Plasma Electron and Current Experiment) instruments.[41] For the ion measurements, here and throughout the paper, the CIS-HIA sensor was used for spacecraft 1 and 3, and the CIS-CODIF sensor for spacecraft 4. HIA is more suitable for measurements in and near the magnetosheath, because CODIF experiences saturation in that region. For spacecraft 4, however, no functioning HIA sensor is available. Cluster 1 and 4 flew close to each other, as can be seen in the orbit plot in Fig. 1. The distance between them was approximately 150 km during these observations. It is seen in Figs. 3 and 4 that the data obtained from these two spacecraft are very similar until they reach the dashed line marking the inner boundary of the transition region, where saturation of the CODIF sensor begins. Thus, the two spacecraft were probing the same plasma, and it is without loss of information that we base the following analysis on only Cluster 1 and 3.

It is seen in Fig. 4 that the plasma inside the magnetosphere has a higher abundance of high energy particles, and a lower density, than the magnetosheath plasma. However, there are isolated patches of magnetosheath plasma also in the magnetosphere. These can also be seen in Figs. 3(j)–3(l) as periods of high density and low temperature (Figs. 3(m)–3(o)). While this magnetosheath plasma is observed, there are also high energy particles present, as is seen in Fig. 4, showing that the spacecraft were located on closed field lines. Fig. 5 shows the density measured by Cluster 1 (black curve) and Cluster 3 (green curve) between 10:39 and
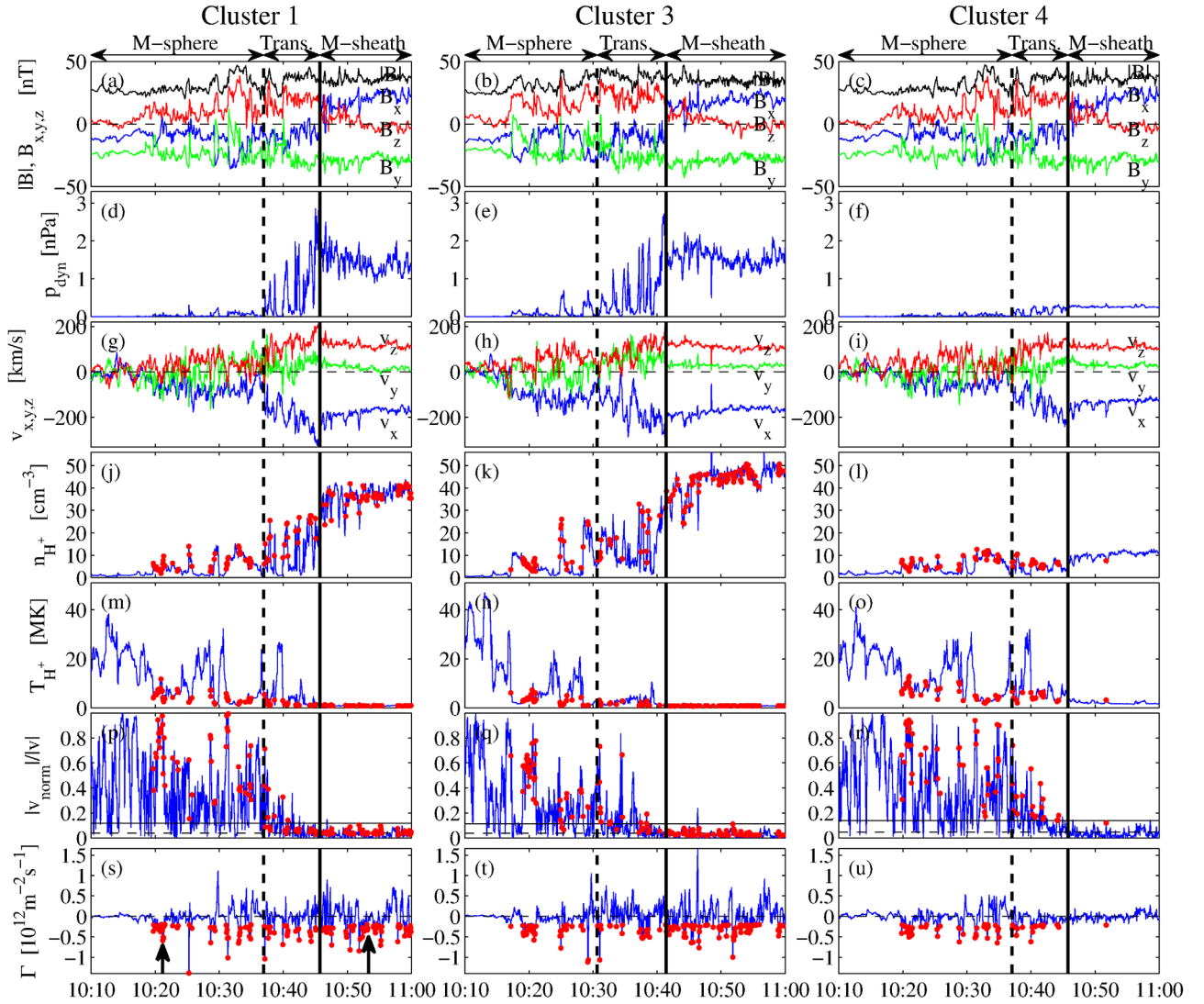
FIG. 3. Data from the Cluster spacecraft on 25 January 2002. The left column shows data from Cluster 1, the middle column Cluster 3, and the right column shows data from Cluster 4. Panels (a-c) show the magnetic field components B_x (blue), B_y (green), B_z (red), and $|\mathbf{B}|$ in nanoteslas. The coordinates are in the GSE system. The curves are labelled at the right hand side of each panel. Panels (d-f) show the dynamic pressure for the three spacecraft, respectively. Panels (g-i) show the velocity components in GSE coordinates: v_x (blue), v_y (green), and v_z (red) in kilometers per second. The curves are labelled at the right hand side of each panel. Panels (j-l) show the proton density. Panels (m-o) show the proton temperature. Panels (p-r) show the ratio of the velocity component normal to the magnetopause $|v_{norm}|$ to the total velocity $|v|$. Panels (s-u) show the cross-magnetopause proton flux perpendicular to the magnetopause Γ. The red dots in panels (j-u) highlight data points with large flux across the magnetopause ($\Gamma < -2 \times 10^{11}$ m^{-2} s^{-1}). In all panels, the dashed and solid vertical lines mark the inner and outer boundaries of the transition region, respectively. The two arrows in panel (s) mark the times for which distribution functions are shown in Fig. 10.

10:43, when Cluster 3 crossed the magnetopause. The density at spacecraft 1 fluctuates between low values that are less than 5 cm^{-3} and high values of approximately 25 cm^{-3}. At the same time, spacecraft 3 measures a steady increase of the density as it moves into the magnetosheath, and the fluctuations that are seen on top of this increase show no correlation with the density at spacecraft 1. Thus, the observations of magnetosheath plasma by Cluster 1, which was in the magnetosphere, were not caused by the magnetopause moving back and forth, since this motion is not seen at Cluster 3, which was located at the magnetopause. That the magnetopause was moving slowly and steadily inwards is also confirmed by the observation that there is only one magnetopause crossing per spacecraft in the magnetic field data, and by the timing of the magnetopause crossings, which is discussed in Sec. IV.

III. PLASMOID MOTION

The measurements presented in Sec. II show that plasma of magnetosheath origin is present on closed magnetic field lines, and that these observations are not caused by an oscillating magnetopause. It rather suggests that plasmoids of finite extent penetrate the magnetopause and that these give rise to the observed fluctuations in density and temperature as they pass by the spacecraft. Fig. 6 shows the ion spectra measured by Cluster 1 and 3 from 10:23 to 10:25. Cluster 3 was closer to the magnetopause than Cluster 1, which was farther inside the magnetosphere. At and around 10:23:30, the density of magnetosheath plasma at Cluster 3 is down to background levels. After a short increase shortly before 10:24, it declines to background levels until it increases again after 10:24:30. During most of this period the density
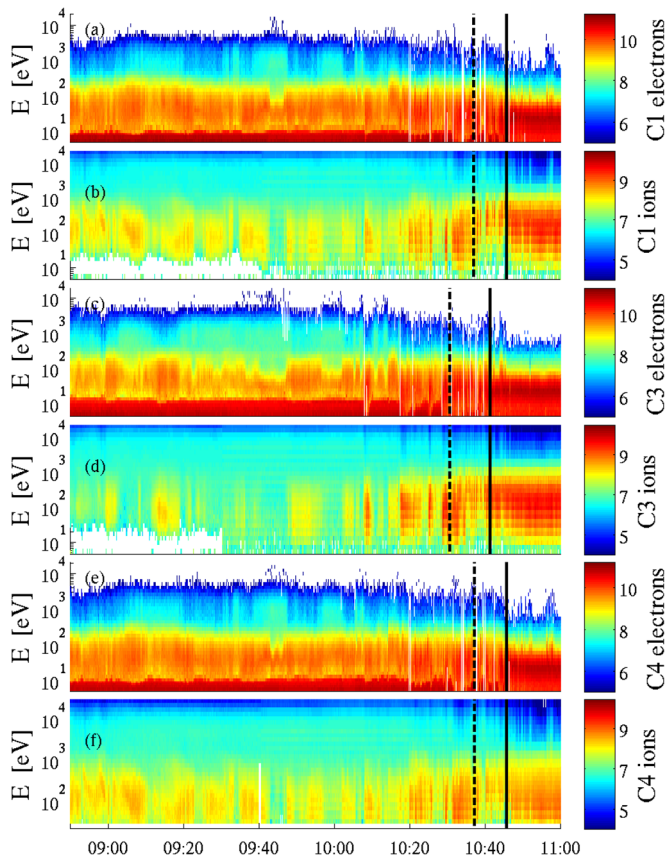
FIG. 4. Field-aligned electron spectrum (a), (c), and (e) for Cluster 1, 3, and 4, respectively. Omnidirectional ion spectrum for Cluster 1, 3, 4 are shown in panels (b), (d), and (f), respectively. The ion spectra for Cluster 1 and 3 were measured by the CIS-HIA sensor, and that for Cluster 4 by CIS-CODIF. The electron spectra were measured by the PEACE instrument. The quantity shown on the color scale is the logarithm of the flux in units of $cm^{-2} \, s^{-1} \, sr^{-1} \, keV^{-1}$. The dashed and solid vertical lines mark the inner and outer boundaries of the transition region, respectively.

of magnetosheath plasma at the inner spacecraft, that is to say at Cluster 1, is well above background level. Thus, a plasmoid was present at the inner spacecraft, but not at the outer, showing that the plasmoids are detached from the magnetopause. This is also illustrated in Fig. 7, which shows the ion temperature along the orbits of Cluster 1 and 3. The magnetopause is shown in the top right corner, where it was
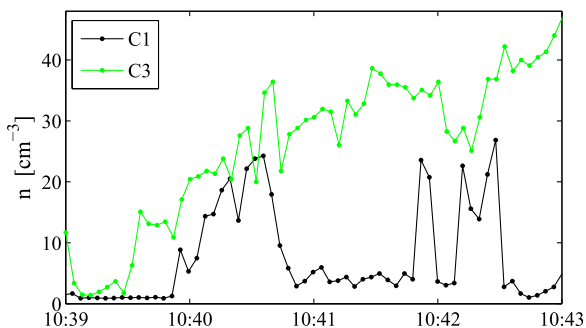

FIG. 5. Density measured by Cluster 1 (black) and by Cluster 3 (green) between 10:39 and 10:43. During this period Cluster 3 crossed the magnetopause, while Cluster 1 was located on the magnetospheric side of it. The magnetopause crossing time for spacecraft 3 was identified in magnetic field data as 10:41:23 UT.
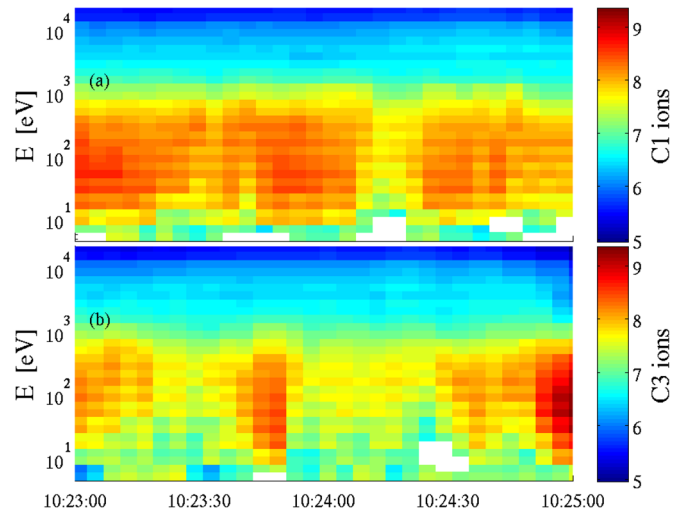

FIG. 6. Closeup of the Cluster 1 (a) and 3 (b) ion spectra from 10:23 to 10:25. Cluster 3 was located closer to the magnetopause and Cluster 1 farther inside the magnetosphere, as is seen by the orbit plot in Fig. 1.

detected by spacecraft 3. The positions of Cluster 1 and 3 at 10:23:58 have been marked in the figure. The two spacecraft followed almost the same track with Cluster 1 approximately 2000 km behind Cluster 3. As in the spectrograms in Fig. 6, it is seen that the temperature is higher at Cluster 3 than at Cluster 1, and that, considering the geometry, the only realistic explanation is that the plasmoids are detached from the magnetopause.

It is possible to trace the plasmoid motion from a spacecraft that is located closer to the magnetopause to one that is located deeper inside the magnetosphere for some of the observed plasmoids. Unless the plasmoid velocity is perfectly aligned with the direction between the spacecraft, the possibility of observing the same plasmoid on two spacecraft will depend on the shape and size of the plasmoid as well as on the angle between the plasmoid velocity and the direction between the spacecraft. Fig. 8 shows the angle α between the plasma velocity measured by Cluster 3 and the direction from Cluster 3 to Cluster 1 (a); the time of flight between the two spacecraft calculated from the velocity measured by Cluster 3 (b); and the densities measured by the two spacecraft (c). The Cluster 3 data in panel (c) and the quantities derived from Cluster 3 data in panels (a) and (b) are shown by green curves. The plasmoids pass Cluster 3 before they reach Cluster 1. Therefore, the spacecraft 3 data, shown by green curves in all panels, have been shifted $\Delta t = 20$ s, corresponding to the dashed black line in panel (b). There is good agreement for both the leading and the trailing edges of the plasmoid that hit Cluster 1 between 10:25 and 10:26, although the density was higher at Cluster 3 than at Cluster 1. The small plasmoid between 10:21 and 10:22 is also predicted fairly well from Cluster 3 data. This is also true for the declining slope around 10:20, when α was around 20°. Before 10:19:40 the density at Cluster 1 was low, while Cluster 3 data would predict a higher density, but here the α-value was much higher, and it is likely that the plasmoid missed spacecraft 1. The distance between the two spacecraft was approximately 2200 km. Thus, the 20 s time of flight
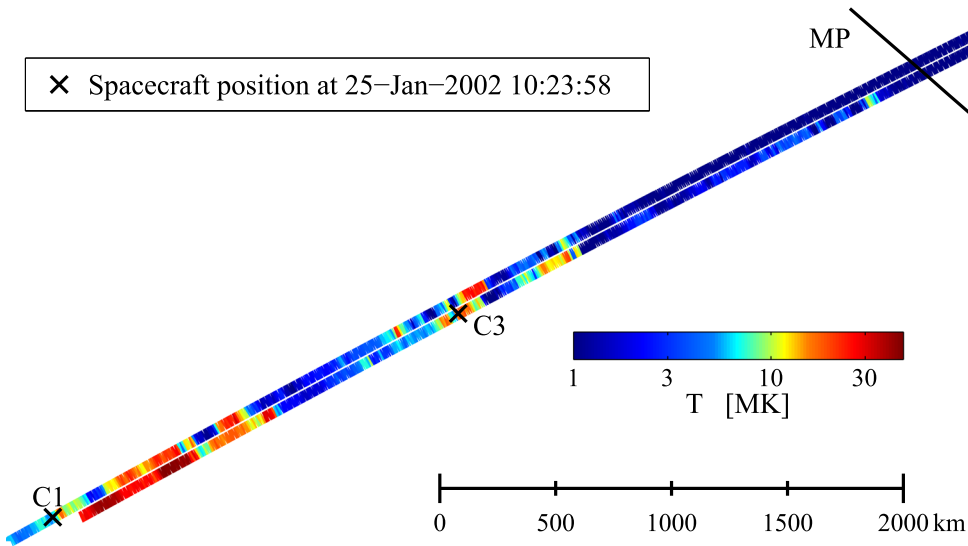
FIG. 7. Color-coded ion temperature along the orbits of Cluster 1 and 3. The spacecraft positions at 10:23:58 have been marked in the figure. The same cylindrical coordinate system as in Fig. 1 is used. Also like in Fig. 1, a scaled Shue model magnetopause is shown in the top right corner in the position where it was encountered by Cluster 3.

corresponds to a plasmoid velocity component of 110 km/s along the spacecraft separation direction.

Figs. 9(a) and 9(b) show the velocity component, measured by CIS, which is perpendicular to the magnetic field for Cluster 1, and 3 (black curves). The perpendicular velocity component decreases as the plasma travels through the transition region. For reference, the drift speed $|\mathbf{E} \times \mathbf{B}|/|\mathbf{B}|^2$ is computed and shown by red dots in Figs. 9(a) and 9(b), using data from the EFW (electric field and waves) instrument.[42] While there is some scatter in the electric field data, the perpendicular velocity component lies within the range of this scatter. The velocity and field data are thus consistent with penetration through polarization of the plasmoid.[12] This is a necessary, but not sufficient, condition for impulsive penetration through polarization. In Figs. 9(c) and 9(d), the perpendicular (black curve) and parallel (blue curve) velocity components are shown. In the vicinity of the magnetopause, the perpendicular component is larger than the parallel component, showing the predominantly perpendicular nature

of the plasma transport. The plasma is seen to slow down as it enters the magnetosphere, bringing the perpendicular velocity down to the same level as the parallel. This slow-down can also be seen in the individual components in Fig. 3.

IV. PARTICLE FLUX ACROSS THE MAGNETOPAUSE

The flux across the magnetopause was computed from the data, and the result is shown in Figs. 3(s)–3(u). The positive direction is defined as outward, and hence the negative flux in the transition region corresponds to plasma moving into the magnetosphere. Peak and mean values of the flux during the last 30 min before each spacecraft reached the magnetopause can be found in Table II. The mean values approximately correspond to 0.2%–0.5%, and the peak values to 20%–24% of the 5.7×10^{12} m^{-2} s^{-1} solar wind flux that was measured by Wind.

The flux was computed in the following way. First, the plasma velocity in the magnetosheath $\mathbf{v}_{MS}$ was determined
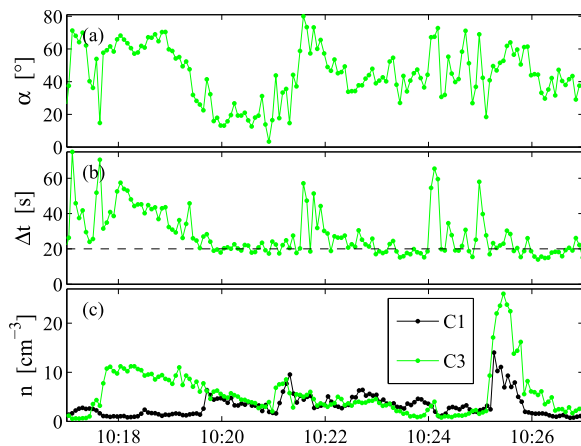

FIG. 8. Panel (a) shows the angle α between the plasma velocity measured by Cluster 3 and the direction from Cluster 3 to Cluster 1. Panel (b) shows the predicted time of flight from spacecraft 3 to 1 based on the velocity measurements by spacecraft 3 (green). Panel (c) shows the density measured by spacecraft 1 (black) and by spacecraft 3 (green). In all panels, the Cluster 3 data, shown by green lines, have been delayed $\Delta t = 20$ s, corresponding to the dashed line in panel (b).
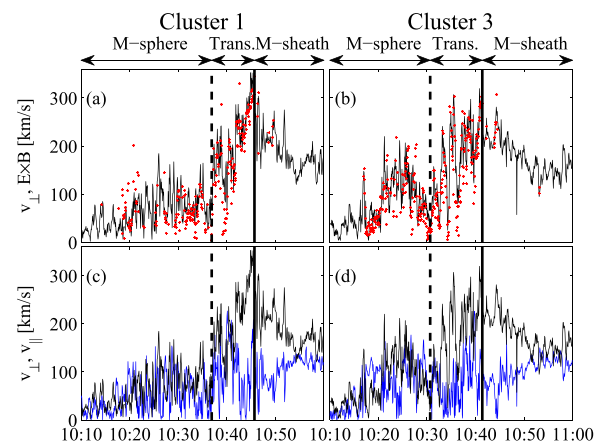

FIG. 9. The upper panels show the perpendicular velocity component $v_\perp$ (black solid curve) for Cluster 1 (a) and Cluster 2 (b). For comparison, $|\mathbf{E} \times \mathbf{B}/B^2|$ is shown by the red dots. The lower panels (c) and (d) show the perpendicular (black curves) and parallel (blue curves) velocity components. The dashed and solid vertical lines mark the inner and outer boundaries of the transition region, respectively.

TABLE II. Mean and peak cross-magnetopause fluxes during the last 30 min before each spacecraft crossed the magnetopause. The two columns with numerical values show the flux calculated by Eqs. (1)–(4) as described in Sec. IV and by using the Shue model with input data from measurements by the Wind spacecraft to compute the magnetopause normal.

	Section IV	Shue
Peak flux C1, $m^{-2}\,s^{-1}$	-1.4×10^{12}	-2.2×10^{12}
Peak flux C3, $m^{-2}\,s^{-1}$	-1.1×10^{12}	-2.1×10^{12}
Mean flux C1, $m^{-2}\,s^{-1}$	-3.0×10^{10}	-6.1×10^{11}
Mean flux C3, $m^{-2}\,s^{-1}$	-1.2×10^{10}	-5.2×10^{11}

by taking the mean value of the velocity during 10 min, starting 2 min after the spacecraft passed the outer boundary of the transition region. The magnetopause is assumed to move with the velocity $\mathbf{v}_{MP}$, which is perpendicular to $\mathbf{v}_{MS}$. The magnitude of $\mathbf{v}_{MP}$ is estimated by

$$|\mathbf{v}_{MP}| = \frac{\mathbf{r}_1 - \mathbf{r}_3}{t_{MP1} - t_{MP3}} \cdot \frac{(\mathbf{v}_{MS} \times \mathbf{r}) \times \mathbf{v}_{MS}}{|(\mathbf{v}_{MS} \times \mathbf{r}) \times \mathbf{v}_{MS}|}, \qquad (1)$$

where t_{MP1} and t_{MP3} are the times when Cluster 1 and 3, respectively, crossed the outer boundary of the transition region, and $\mathbf{r}_1$ and $\mathbf{r}_3$ are the corresponding positions in GSE coordinates. The estimate was carried out for each spacecraft, and $\mathbf{r}$ without subscript is taken to be the position of the spacecraft in question at the time of the crossing of the outer boundary. The inclusion of $\mathbf{r}$ in the double vector product in Eq. (1) serves to remove the azimuthal component of the magnetopause velocity, i.e., a cylindrically symmetric magnetopause is assumed. The axis of symmetry can be computed from the data and is approximately anti-parallel to the solar wind velocity. For example, the axis of symmetry computed from Cluster 3 data is in the (0.965, 0.261, 0) direction, which is $6.4°$ from being anti-parallel to the solar wind velocity in Table I. For Cluster 1 and 3, we obtain $|\mathbf{v}_{MP}| \approx 4.8$ km/s and 4.5 km/s, respectively. The flux values were calculated in this moving frame of reference. In a frame of reference where the magnetopause is at rest, the plasma velocity in the magnetosheath is parallel to the magnetopause. In the GSE frame, we subtract $\mathbf{v}_{MP}$ from $\mathbf{v}_{MS}$ and normalize to obtain a unit vector $\hat{v}_{tan}$.

$$\hat{v}_{tan} = \frac{\mathbf{v}_{MS} - \mathbf{v}_{MP}}{|\mathbf{v}_{MS} - \mathbf{v}_{MP}|}. \qquad (2)$$

We calculate the plasma flux along the magnetopause normal, which is

$$\hat{N} = \frac{(\hat{v}_{tan} \times \mathbf{r}) \times \hat{v}_{tan}}{|(\hat{v}_{tan} \times \mathbf{r}) \times \hat{v}_{tan}|}, \qquad (3)$$

and we obtain $\hat{N} = (0.51, 0.57, 0.64)$ for Cluster 1 and $\hat{N} = (0.53, 0.57, 0.64)$ for Cluster 3. Finally, the flux, in the frame of the moving magnetopause, is found using

$$\Gamma = n(\mathbf{v} - \mathbf{v}_{MP}) \cdot \hat{N}. \qquad (4)$$

To verify the significance of the computed flux, we computed the ratio $|\mathbf{v} \cdot \hat{N}|/|\mathbf{v}|$ of the normal component of the velocity to the magnitude of the velocity. This is shown in Figs. 3(p)–3(r). With the definition of the normal above, the velocity in the magnetosheath should be purely tangential. Hence, all the non-zero values of $|\mathbf{v} \cdot \hat{N}|/|\mathbf{v}|$ in the magnetosheath can be seen as noise. In Figs. 3(p)–3(r), the root mean square value of $|\mathbf{v} \cdot \hat{N}|/|\mathbf{v}|$ in the magnetosheath is shown by a horizontal dashed line, and three times the root mean square by a horizontal solid line. As expected, these values are low.

Data points with a large inward flux ($\Gamma < -2 \times 10^{11}$ $m^{-2}\,s^{-1}$) have been marked by dots in Figs. 3(s)–3(u). The corresponding dots in Figs. 3(p)–3(r) show that $|\mathbf{v} \cdot \hat{N}|/|\mathbf{v}|$ was above the level of the magnetosheath noise for data points with a large inward flux everywhere until the spacecraft reached the inner boundary of the transition region (shown by the vertical dashed line). Further verification of the significance of these results is obtained from Fig. 10, in which distribution functions measured by Cluster 1 are shown for the two times that are marked by arrows in Fig. 3(s). The horizontal axes correspond to the direction normal to the magnetopause and the vertical axes to the $\hat{v}_{tan}$-direction, which is parallel to the magnetosheath plasma flow. The vector $\hat{v}_{tan}$ is defined in Eq. (2). The left hand panel shows the distribution function at 10:21:11, when the spacecraft was located inside the magnetosphere and a large inward flux was measured, as is seen in Fig. 3(s). The distribution function is observed to be centred on a velocity anti-parallel to the magnetopause normal. In the right hand panel, an example of a magnetosheath distribution is shown. There, the distribution is displaced vertically in the figure showing that the flow was tangential to the magnetopause.

Determining the direction of the magnetopause normal from the plasma velocity in the magnetosheath, we consider the magnetopause to be the object around which the magnetosheath plasma flows. It is seen from Fig. 3 that the velocity in the magnetosheath is fairly constant, and by determining the normal from data taken there, we avoid the larger fluctuations of the transition region, where the magnetopause orientation may be fluctuating. Indeed, the magnetopause itself may not be clearly defined during the penetration process. The mean flux values in Table II show that there is a net flux of plasma from the magnetosheath, across the transition region, and into the magnetosphere.

For comparison we also computed the flux using the Shue model,[35] with the solar wind parameters in Table I as input, to estimate the direction of the normal of the magnetopause. The normal according to the Shue model is (0.69, 0.44, 0.58). The peak fluxes thus obtained are greater than those calculated according to Eqs. (1)–(4) by about a factor of two, and the mean fluxes are an order of magnitude higher. When the Shue model normal is used, a non-zero mean flux is obtained in the magnetosheath. The Shue model gives an average shape of the magnetopause, but it does not provide a good estimate of the magnetopause normal on one particular occasion. Therefore, the normal from obtained in Eq. (3) gives better flux estimates. Mean and peak fluxes for the Shue model magnetopause using Wind data as inputs are shown in Table II together with those that were obtained using Eqs. (1)–(4).
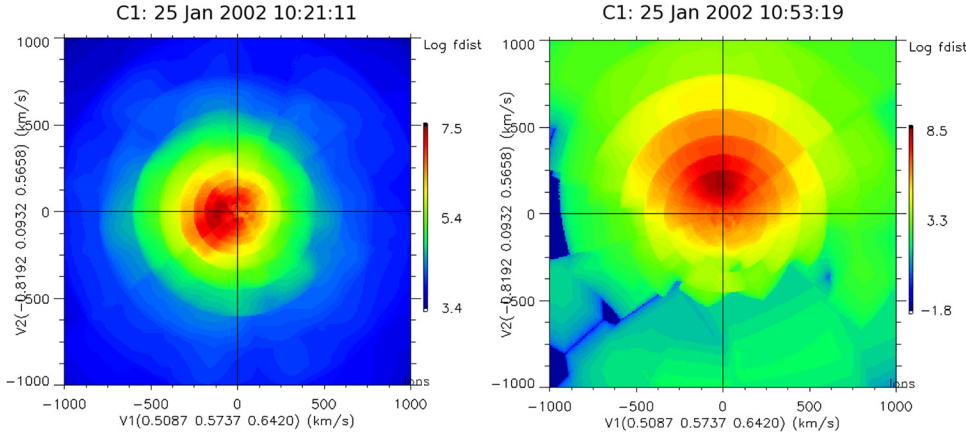
FIG. 10. Velocity distribution functions for Cluster 1 at 10:21:11 (left) and 10:53:19 (right). The horizontal axis shows the velocity component normal to the magnetopause, and the vertical axis shows the tangential component parallel to the magnetosheath flow direction. The observation times are marked by arrows in panel (s) of Fig. 3.

There are fluctuations on the flux in the magnetosheath and in the transition region. Farther into the magnetosphere the inward direction dominates more and more (Figs. 3(s)–3(u)). That the values of the mean flux in Table II are negative shows that the magnetopause is on average being penetrated by plasma from the magnetosheath. The large inward flux data points in Figs. 3(s)–3(u) have also been marked in the density (Figs. 3(j)–3(l)) and temperature (Figs. 3(m)–3(o)) diagrams, showing that periods of large inward flux are characterized by high density and low temperature. This is also seen in the particle spectra shown in Fig. 4. There are data points where there is no large flux, but the temperature is relatively low, indicating the presence of a background of stationary low temperature plasma, which can also be seen in particle spectra. In Figs. 3(s)–3(u), it is seen that a significant inward flux is observed as early as 10:17 by Cluster 3 and at 10:20 by Cluster 1. At these times, the spacecraft were located approximately half an earth radius inside the point where they later entered the magnetosheath. At earlier times, the flux tends to zero, as does the velocity. The distance to the magnetopause can be seen in Fig. 7, where the spacecraft positions at 10:24 are marked.

directions used in panels (a) and (b) were then defined by the vector product $\hat{u}_1 = \hat{N}_{\mathrm{MVA}} \times (0, 1, 0)$ and those in panels (c) and (d) by $\hat{u}_2 = \hat{u}_1 \times \hat{N}_{\mathrm{MVA}}$.

For the curves shown in panels (a) and (b), for Cluster 1 and 3, respectively, the agreement between Δv and $\Delta B / \sqrt{\mu_0 n m_p}$ is quite good in the magnetosheath, and in a thin layer on the inside of the magnetopause for both the spacecraft. This layer was traversed by the spacecraft during the last 40–50 s before they reached the magnetopause. Elsewhere inside the magnetopause no agreement is seen for either of the spacecraft. In the lower panels (c) and (d), which show Δv and $-\Delta B / \sqrt{\mu_0 n m_p}$, there is agreement between the two curves for some features in the magnetosheath, but that agreement does not reach across the magnetopause. These observations are consistent with the presence of a reconnection jet on the inside of the magnetopause. However, reconnection only couples the plasma on the magnetosheath side of the magnetopause to a thin sheath on the magnetospheric side. This is seen in Fig. 11, and it is also what is predicted by theory, simulations, and experiments on magnetic reconnection [see review by Ref. 44].
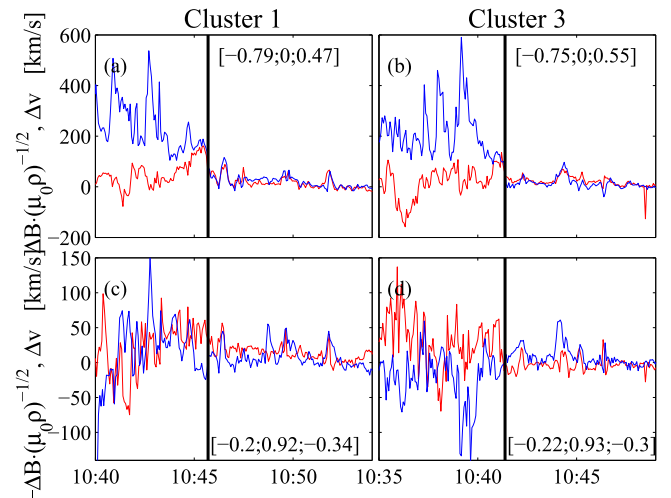
V. ROTATIONAL DISCONTINUITY TEST

In MHD theory of reconnection, the boundary where reconnection is happening is a rotational discontinuity. The plasmas on both sides of the discontinuity are magnetically connected, and the flow acceleration is predicted to be Alfvénic.[43] We use the test described by Phan *et al.*[43] in their Sec. 4.1 to find whether or not the magnetopause is a rotational discontinuity. The results are shown in Fig. 11. We plot the change in the velocity components (red curves) in two tangential directions as indicated in each panel. The tangential velocity components are compared with the change in the corresponding tangential magnetic field components divided by $\sqrt{\mu_0 n m_p}$ (blue curves). As reference points we use the values obtained 7 min after each spacecraft entered the magnetosheath. The local magnetopause normal was determined by a minimum variance analysis of the magnetic field, and was found to be $\hat{N}_{\mathrm{MVA}} = (0.47, 0.40, 0.79)$ for Cluster 1 and $\hat{N}_{\mathrm{MVA}} = (0.55, 0.37, 0.75)$ for Cluster 3. Both these normals differ by $13°$ from the average normals found in Sec. IV for Cluster 1 and 3, respectively. The tangential

FIG. 11. Rotational discontinuity test. The red curves show Δv in the direction indicated in each panel. The blue curves show $\Delta B / \sqrt{\mu_0 n m_p}$ in the same direction in panels (a) and (b), and $-\Delta B / \sqrt{\mu_0 n m_p}$ in panels (c) and (d). Cluster 1 results are shown in panels (a) and (c) and Cluster 3 in panels (b) and (d).

VI. PLASMOID SIZE

Limits of the cross-field width of plasmoids that can penetrate through polarization appear in the literature,[45] and large plasmoids have been seen to break up into smaller plasmoids in laboratory experiments.[16] It is therefore interesting to estimate the width of the plasmoids that are observed here.

For the cross-field distance between two spacecraft, m and n, we use the projection of the distance between spacecraft on the direction of the polarization electric field. This can be estimated by

$$d_{m,n} = \frac{|(\mathbf{r}_n - \mathbf{r}_m) \cdot \mathbf{v}_m \times \mathbf{B}_m|}{|\mathbf{v}_m \times \mathbf{B}_m|},$$

where $\mathbf{r}_{m,n}$ is the spacecraft position; and $\mathbf{v}_m$ and $\mathbf{B}_m$ are, respectively, the velocity and magnetic field measured by spacecraft m. Taking the mean value of this distance over the time Cluster 1 spent in the transition region, we obtain $d_{1,3} \approx 1400$ km and $d_{1,4} \approx 140$ km. As we observed in Sec. II, the data from Cluster 1 and 4 are very similar, showing that these spacecraft passed through the same plasmoids. The plasmoid width w is thus expected to be much larger than 140 km. The agreement between Cluster 3 and the other two is not as good, indicating that it observes the same plasmoids as the other spacecraft some of the time, but not all of the time, and therefore $d_{1,3} \approx 1400$ km may serve as an order of magnitude estimate of w. Estimating the kinetic beta at the magnetopause from the last data point on the inside of the outer boundary of the transition region, we arrive at $\beta_k = 4.5$ for both Cluster 1 and Cluster 3. With these parameters, the boundary between the expulsion and polarization regions in the theory by Brenning *et al.*[45] is at $w \approx 30$ km. Since our estimate is that the plasmoids are much larger than 140 km, their theory predicts that penetration should occur through expulsion in the present case.

Plasmoids could penetrate through an expulsion of the ambient magnetic field, which is followed by a magnetic diffusion and a convection phase, as outlined by Wessel *et al.*[14] A combination of polarization and expulsion is also possible.[45] Comparing the magnitude of the magnetic field in Figs. 3(a)–3(c) (black curve) and the density in Figs. 3(j)–3(l) it is possible to find plasmoids, for which the magnetic field magnitude inside is higher, that is to say, closer to magnetosheath values, than in the surrounding plasma, for example, the plasmoid that is seen by Cluster 1 and 3 at 10:25. However, there are also plasmoids that do not have a clear magnetic signature. Thus, we cannot clearly distinguish between expulsion and polarization, and since both can occur at the same time,[45] it may not always be possible to make such a distinction. The dependence of the penetration on plasmoid size remains an open question, which is a suitable topic for laboratory experiments and simulations, as well as further multi-spacecraft measurements.

VII. CONCLUSIONS AND DISCUSSION

We have presented data from the Cluster satellites, showing a plasma flux from the magnetosheath into the magnetosphere. Plasma with the characteristics of the magnetosheath, i.e., lower temperature and higher density than the magnetospheric plasma, is seen in the magnetosphere, and as far inside as half an earth radius from the magnetopause an inward flux is observed. It is seen from the particle spectra and from the density and temperature diagrams that the magnetosheath plasma enters the magnetosheath as plasmoids of finite extent. We can trace plasmoids moving from one spacecraft to the next and find good agreement between the plasmoid time of flight and the measured plasma velocity. The magnetic field magnitude inside the plasmoids is closer to the values in the magnetosheath than the surrounding plasma in some, but not all, cases. The cross-field width of the plasmoids is much greater than 140 km, and the cross-field distance between spacecraft 1 and 3 of 1400 km will serve as an order of magnitude estimate. These observations are consistent with plasma entry through impulsive penetration,[9] where the plasmoids enter by both expulsion of the local magnetic field and by polarization[14] or a combination of the two.[45]

Although we interpret our observations in terms of impulsive penetration, the applicability to this case of other models that have been proposed in the literature deserves a brief discussion. Impulsive reconnection on the dayside magnetopause in flux transfer events[3,4] can connect field lines that previously were closed to open solar wind field lines. Then solar wind plasma can enter along these field lines, creating field-aligned beams and magnetic bubbles in the process.[46] As proposed by Dungey,[47] the plasma thus entered remains magnetically connected to the magnetosheath plasma moving with it toward the tail where reconnection again can form closed field lines, on which the newly entered plasma becomes trapped. Subsequently, in Dungey's picture, the plasma that entered while the field lines were open flows back around the earth, populating the dayside magnetosphere. While it is likely that reconnection is happening during our observations, it cannot explain these, because we measure plasma transport straight through the magnetosphere on the dayside, rather than plasma taking the long road via the cusp and the tail.

Reconnection can also occur in the magnetospheric lobes, particularly for a northerly directed interplanetary magnetic field,[5] and this process can attach fluxtubes containing magnetosheath plasma to the outside of the dayside magnetopause, creating a thick boundary layer. This process does, however, require a strong northward interplanetary magnetic field,[6] and in the present case the northward component of the interplanetary magnetic field was much smaller than the component in the ecliptic plane.

The Kelvin-Helmholtz instability is thought to be responsible for transport of plasma into the magnetosphere along its flanks at the terminator plane and further downstream in the tail. However, to cause transport, it would need to reach a non-linear stage, which is unlikely at the dayside magnetopause.[7,8] In the vortices that form in the non-linear stage of the instability, low density plasma moves tailward faster than the magnetosheath plasma.[48] We do not observe this, nor the periodic signatures that would be expected from the instability in both the linear and non-linear stages. On the

contrary, the magnetopause is not oscillating, as is seen in magnetic data, where each spacecraft crosses the magnetopause only once, and by the steady increase in density that is measured as the spacecraft move across the magnetopause. We conclude that the Kelvin-Helmholtz instability is not responsible for the plasma transport reported here.

Cluster data from the same period of time that is presented here have previously been analysed by Fear *et al.*[2] In their interpretation, the spacecraft approached a smooth gradient intermittently, due to oscillations in the magnetopause position. That interpretation is consistent with the observations only when each spacecraft is viewed separately. Using simultaneous measurements on two of the Cluster spacecraft it is seen, in Fig. 5, that the magnetopause was moving slowly and only in the inward direction. Thus, the large fluctuations on the spacecraft in the magnetosphere were not caused by magnetopause motion. Instead, they were caused by plasmoids of magnetosheath plasma that had penetrated the magnetopause. With simultaneous measurements on two spacecraft, the inward plasmoid motion can be traced (Fig. 8) from one spacecraft to the next. The direction of the velocity of the plasmoids traced in this way shows that they came from the magnetopause, and by simultaneous measurements of the ion spectra it is seen that they are detached from it (Figs. 6 and 7).

Fig. 12 shows a sketch of the plasmoid motion. In the magnetosheath, the plasmoids move predominantly in a tangential direction with respect to the magnetopause. Superimposed on the tangential motion some plasmoids have an inward and some an outward velocity component along the magnetopause normal. Further in, the motion is increasingly directed inwards, because only plasmoids with a large inward velocity can reach that far in that direction. Inward

moving plasmoids that are detached from the magnetopause are seen inside the magnetosphere. The plasmoids slow down as they enter the magnetosphere, and once they have stopped they are likely to stay there and contribute to the magnetospheric plasma density. In summary, by observing plasmoids of magnetosheath origin penetrating the magnetopause, we have shown that the impulsive penetration mechanism, which is known from laboratory experiments on magnetic barriers, also is active in space.
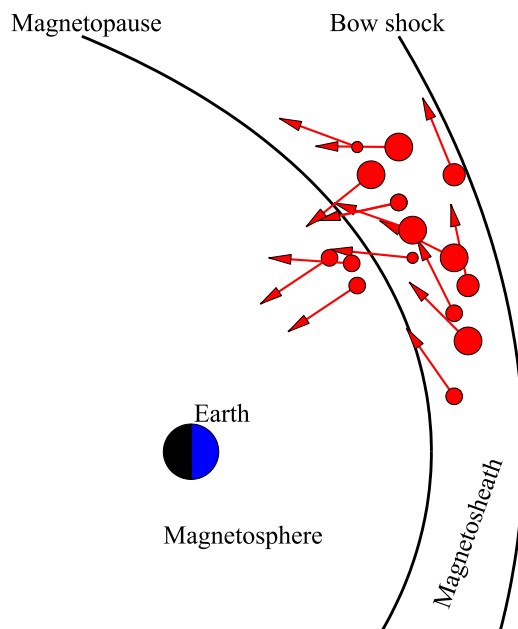
ACKNOWLEDGMENTS

FIG. 12. A sketch of the plasmoid motion. In the magnetosheath, plasmoids move mostly parallel to the magnetopause, but with an overlaid component inward along the normal direction. Further in, the direction of motion is increasingly inward.

[1]S.-I. Akasofu, Space Sci. Rev. **28**, 121 (1981).
[2]R. C. Fear, A. N. Fazakerley, C. J. Owen, A. D. Lahiff, E. A. Lucek, A. Balogh, L. M. Kistler, C. Mouikis, and H. Rème, Ann. Geophys. **23**, 2605 (2005).
[3]C. T. Russell and R. C. Elphic, Space Sci. Rev. **22**, 681 (1978).
[4]C. T. Russell and R. C. Elphic, Geophys. Res. Lett. **6**, 33, doi:10.1029/GL006i001p00033 (1979).
[5]J. T. Gosling, M. F. Thomsen, S. J. Bame, R. C. Elphic, and C. T. Russell, J. Geophys. Res. **96**, 14097, doi:10.1029/91JA01139 (1991).
[6]P. Song and C. T. Russell, J. Geophys. Res. **97**, 1411, doi:10.1029/91JA02377 (1992).
[7]D. Sibeck, G. Paschmann, R. Treumann, S. Fuselier, W. Lennartsson, M. Lockwood, R. Lundin, K. Ogilvie, T. Onsager, T.-D. Phan, M. Roth, M. Scholer, N. Sckopke, K. Stasiewicz, and M. Yamauchi, Space Sci. Rev. **88**, 207 (1999).
[8]H. Hasegawa, M. Fujimoto, T.-D. Phan, H. Rème, A. Balogh, M. W. Dunlop, C. Hashimoto, and R. TanDokoro, Nature (London) **430**, 755 (2004).
[9]J. Lemaire, Planet. Space Sci. **25**, 887 (1977).
[10]W. H. Bostick, Phys. Rev. **104**, 292 (1956).
[11]*The Oxford English Dictionary*, 2nd ed., edited by J. Simpson and E. Weiner (Oxford University Press, Oxford, 1989).
[12]G. Schmidt, Phys. Fluids **3**, 961 (1960).
[13]W. Peter and N. Rostoker, Phys. Fluids **25**, 730 (1982).
[14]F. J. Wessel, R. Hong, J. Song, A. Fisher, N. Rostoker, A. Ron, R. Li, and R. Y. Fan, Phys. Fluids **31**, 3778 (1988).
[15]H. Ishizuka and S. Robertson, Phys. Fluids **25**, 2353 (1982).
[16]B. H. Ripin, E. A. McLean, C. K. Manka, C. Pawley, J. A. Stamper, T. A. Peyser, A. N. Mostovych, J. Grun, and J. Huba, Phys. Rev. Lett. **59**, 2299 (1987).
[17]A. B. Hassam and J. D. Huba, Geophys. Res. Lett. **14**, 60, doi:10.1029/GL014i001p00060 (1987).
[18]B. Häusler, R. A. Treumann, O. H. Bauer, G. Haerendel, R. Bush, C. W. Carlsson, B. Theile, M. C. Kelley, V. S. Dokunin, and Y. Y. Ruzhin, J. Geophys. Res. **91**, 287, doi:10.1029/JA091iA01p00287 (1986).
[19]J. Lemaire, J. Plasma Phys. **33**, 425 (1985).
[20]M. M. Echim, J. F. Lemaire, and M. Roth, Phys. Plasmas **12**, 072904 (2005).
[21]T. Hurtig, N. Brenning, and M. A. Raadu, Phys. Plasmas **10**, 4291 (2003).
[22]T. Hurtig, N. Brenning, and M. A. Raadu, Phys. Plasmas **11**, L33 (2004).
[23]H. Gunell, T. Hurtig, H. Nilsson, M. Koepke, and N. Brenning, Plasma Phys. Controlled Fusion **50**, 074013 (2008).
[24]H. Gunell, J. J. Walker, M. E. Koepke, T. Hurtig, N. Brenning, and H. Nilsson, Phys. Plasmas **16**, 112901 (2009).
[25]M. André, R. Behlke, J.-E. Wahlund, A. Vaivads, A.-I. Eriksson, A. Tjulin, T. D. Carozzi, C. Cully, G. Gustafsson, D. Sundkvist, Y. Khotyaintsev, N. Cornilleau-Wehrlin, L. Rezeau, M. Maksimovic, E. Lucek, A. Balogh, M. Dunlop, P.-A. Lindqvist, F. Mozer, A. Pedersen, and A. Fazakerley, Ann. Geophys. **19**, 1471 (2001).
[26]J. Woch and R. Lundin, J. Geophys. Res. **97**, 1431, doi:10.1029/91JA02490 (1992).
[27]R. Lundin, J.-A. Sauvaud, H. Rème, A. Balogh, I. Dandouras, J. M. Bosqued, C. Carlson, G. K. Parks, E. Möbius, L. M. Kistler, B. Klecker,

E. Amata, V. Formisano, M. Dunlop, L. Eliasson, A. Korth, B. Lavraud, and M. McCarthy, Ann. Geophys. **21**, 457 (2003).

[28]D. Hubert, C. Perche, C. C. Harvey, C. Lacombe, and C. T. Russell, Geophys. Res. Lett. **16**, 159, doi:10.1029/GL016i002p00159 (1989).

[29]S. Savin, L. Zelenyi, E. Amata, J. Buechner, J. Blecki, A. Greco, S. Klimov, R. E. Lopez, B. Nikutowski, E. Panov, J. Pickett, J. L. Rauch, S. Romanov, P. Song, A. Skalsky, V. Smirnov, A. Taktakishvili, P. Veltry, and G. Zimbardo, Planet. Space Sci. **53**, 133 (2005).

[30]S. Savin, E. Amata, L. Zelenyi, V. Budaev, G. Consolini, R. Treumann, E. Lucek, J. Safrankova, Z. Nemecek, Y. Khotyaintsev, M. Andre, J. Buechner, H. Alleyne, P. Song, J. Blecki, J. L. Rauch, S. Romanov, S. Klimov, and A. Skalsky, JETP Lett. **87**, 593 (2008).

[31]S. Savin, V. Budaev, L. Zelenyi, E. Amata, D. Sibeck, V. Lutsenko, N. Borodkova, H. Zhang, V. Angelopoulos, J. Safrankova, Z. Nemecek, J. Blecki, J. Buechner, L. Kozak, S. Romanov, A. Skalsky, and V. Krasnoselskikh, JETP Lett. **93**, 754 (2011).

[32]H. Hietala, N. Partamies, T. V. Laitinen, L. B. N. Clausen, G. Facskó, A. Vaivads, H. E. J. Koskinen, I. Dandouras, H. Rème, and E. A. Lucek, Ann. Geophys. **30**, 33 (2012).

[33]T. Karlsson, N. Brenning, H. Nilsson, J.-G. Trotignon, X. Vallières, and G. Facsko, J. Geophys. Res. **117**, A03227, doi:10.1029/2011JA017059 (2012).

[34]E. V. Mishin, P. A. Puhl-Quinn, and O. Santolik, Geophys. Res. Lett. **37**, L07106, doi:10.1029/2010GL042929 (2010).

[35]J. Shue, J. K. Chao, H. C. Fu, C. T. Russell, P. Song, K. K. Khurana, and H. J. Singer, J. Geophys. Res. **102**, 9497, doi:10.1029/97JA00196 (1997).

[36]R. P. Lepping, M. H. Acũna, L. F. Burlaga, W. M. Farrell, J. A. Slavin, K. H. Schatten, F. Mariani, N. F. Ness, F. M. Neubauer, Y. C. Whang, J. B. Byrnes, R. S. Kennon, P. V. Panetta, J. Scheifele, and E. M. Worley, Space Sci. Rev. **71**, 207 (1995).

[37]K. W. Ogilvie, D. J. Chornay, R. J. Fritzenreiter, F. Hunsaker, J. Keller, J. Lobell, G. Miller, J. D. Scudder, E. C. Sittler, Jr., R. B. Torbert, D. Bodet, G. Needell, A. J. Lazarus, J. T. Steinberg, J. H. Tappan, A. Mavretic, and E. Gergin, Space Sci. Rev. **71**, 55 (1995).

[38]A. Balogh, C. M. Carr, M. H. Acũna, M. W. Dunlop, T. J. Beek, P. Brown, K.-H. Fornaçon, E. Georgescu, K.-H. Glassmeier, J. Harris, G. Musmann, T. Oddy, and K. Schwingenschuh, Ann. Geophys. **19**, 1207 (2001).

[39]D. G. Mitchell, F. Kutchko, D. J. Williams, T. E. Eastman, and L. A. Frank, J. Geophys. Res. **92**, 7394, doi:10.1029/JA092iA07p07394 (1987).

[40]H. Rème, C. Aoustin, J. M. Bosqued, I. Dandouras, B. Lavraud, J. A. Sauvaud, A. Barthe, J. Bouyssou, T. Camus, O. Coeur-Joly, A. Cros, J. Cuvilo, F. Ducay, Y. Garbarowitz, J. L. Medale, E. Penou, H. Perrier, D. Romefort, J. Rouzaud, C. Vallat, D. Alcaydé, C. Jacquey, C. Mazelle, C. D'Uston, E. Möbius, L. M. Kistler, K. Crocker, M. Granoff, C. Mouikis, M. Popecki, M. Vosbury, B. Klecker, D. Hovestadt, H. Kucharek, E. Kuenneth, G. Paschmann, M. Scholer, N. Sckopke, E. Seidenschwang, C. W. Carlson, D. W. Curtis, C. Ingraham, R. P. Lin, J. P. McFadden, G. K. Parks, T. Phan, V. Formisano, E. Amata, M. B. Bavassano-Cattaneo, P. Baldetti, R. Bruno, G. Chionchio, A. di Lellis, M. F. Marcucci, G. Pallocchia, A. Korth, P. W. Daly, B. Graeve, H. Rosenbauer, V. Vasyliunas, M. McCarthy, M. Wilber, L. Eliasson, R. Lundin, S. Olsen, E. G. Shelley, S. Fuselier, A. G. Ghielmetti, W. Lennartsson, C. P. Escoubet, H. Balsiger, R. Friedel, J.-B. Cao, R. A. Kovrazhkin, I. Papamastorakis, R. Pellat, J. Scudder, and B. Sonnerup, Ann. Geophys. **19**, 1303 (2001).

[41]A. D. Johnstone, C. Alsop, S. Burge, P. J. Carter, A. J. Coates, A. J. Coker, A. N. Fazakerley, M. Grande, R. A. Gowen, C. Gurgiolo, B. K. Hancock, B. Narheim, A. Preece, P. H. Sheather, J. D. Winningham, and R. D. Woodliffe, Space Sci. Rev. **79**, 351 (1997).

[42]G. Gustafsson, M. André, T. Carozzi, A. I. Eriksson, C.-G. Fälthammar, R. Grard, G. Holmgren, J. A. Holtet, N. Ivchenko, T. Karlsson, Y. Khotyaintsev, S. Klimov, H. Laakso, P.-A. Lindqvist, B. Lybekk, G. Marklund, F. Mozer, K. Mursula, A. Pedersen, B. Popielawska, S. Savin, K. Stasiewicz, P. Tanskanen, A. Vaivads, and J.-E. Wahlund, Ann. Geophys. **19**, 1219 (2001).

[43]T. Phan, M. Dunlop, G. Paschmann, B. Klecker, J. Bosqued, H. Rème, A. Balogh, C. Twitty, F. Mozer, C. Carlson, C. Mouikis, and L. Kistler, Ann. Geophys. **22**, 2355 (2004).

[44]M. Yamada, R. Kulsrud, and H. Ji, Rev. Mod. Phys. **82**, 603 (2010).

[45]N. Brenning, T. Hurtig, and M. A. Raadu, Phys. Plasmas **12**, 012309 (2005).

[46]D. J. Southwood, C. J. Farrugia, and M. A. Saunders, Planet. Space Sci. **36**, 503 (1988).

[47]J. W. Dungey, Phys. Rev. Lett. **6**, 47 (1961).

[48]H. Hasegawa, M. Fujimoto, K. Takagi, Y. Saito, T. Mukai, and H. Rème, J. Geophys. Res., [Space Phys.] **111**, 9203, doi:10.1029/2006JA011728 (2006).